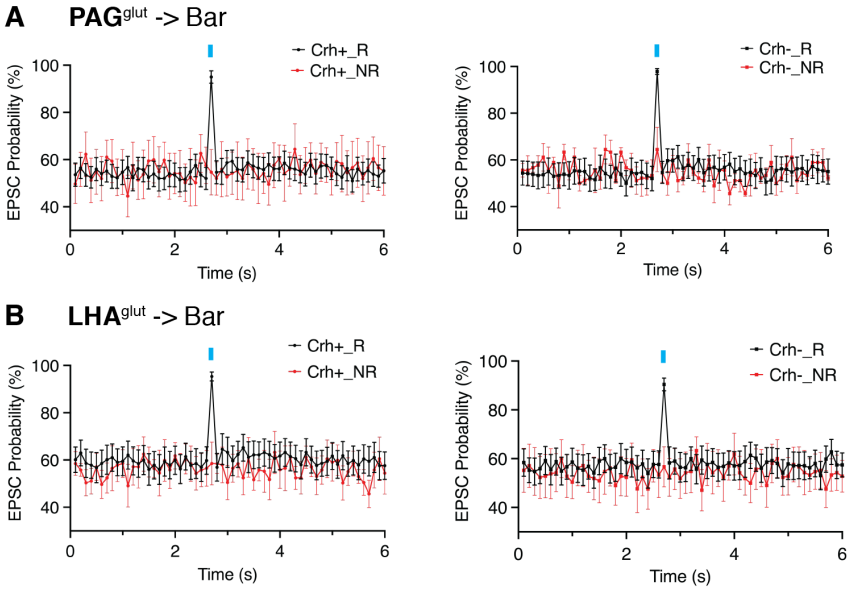

Figure S1. Glutamatergic PAG and LHA neurons are functionally connected to Bar. Related to Figure 1.

A) Average EPSC probability of Bar$^{Crh/Vglut2}$ (n = 28) or Bar$^{Crh\text{-}negative}$ (n = 20) neurons that responded and Bar$^{Crh/Vglut2}$ (n = 7) or Bar$^{Crh\text{-}negative}$ (n = 5) neurons that did not respond to photostimulation *in vitro*, of the vlPAG input.
B) Average EPSC probability of Bar$^{Crh/Vglut2}$ (left panel, n = 20) or Bar$^{Crh\text{-}negative}$ (right panel, n = 17) neurons that responded (R), and Bar$^{Crh/Vglut2}$ (n = 5) or Bar$^{Crh\text{-}negative}$ (n = 7) neurons that did not respond (NR) to photostimulation of the LHA input.

Blue bars at the top of the recording traces indicate 10 ms blue light pulse stimulation. Group data are presented as population mean ± s.e.m. *Abbreviations: Bar, Barrington's Nucleus; LHA, lateral hypothalamic area; PAG, periaqueductal gray; vl, ventrolateral.*

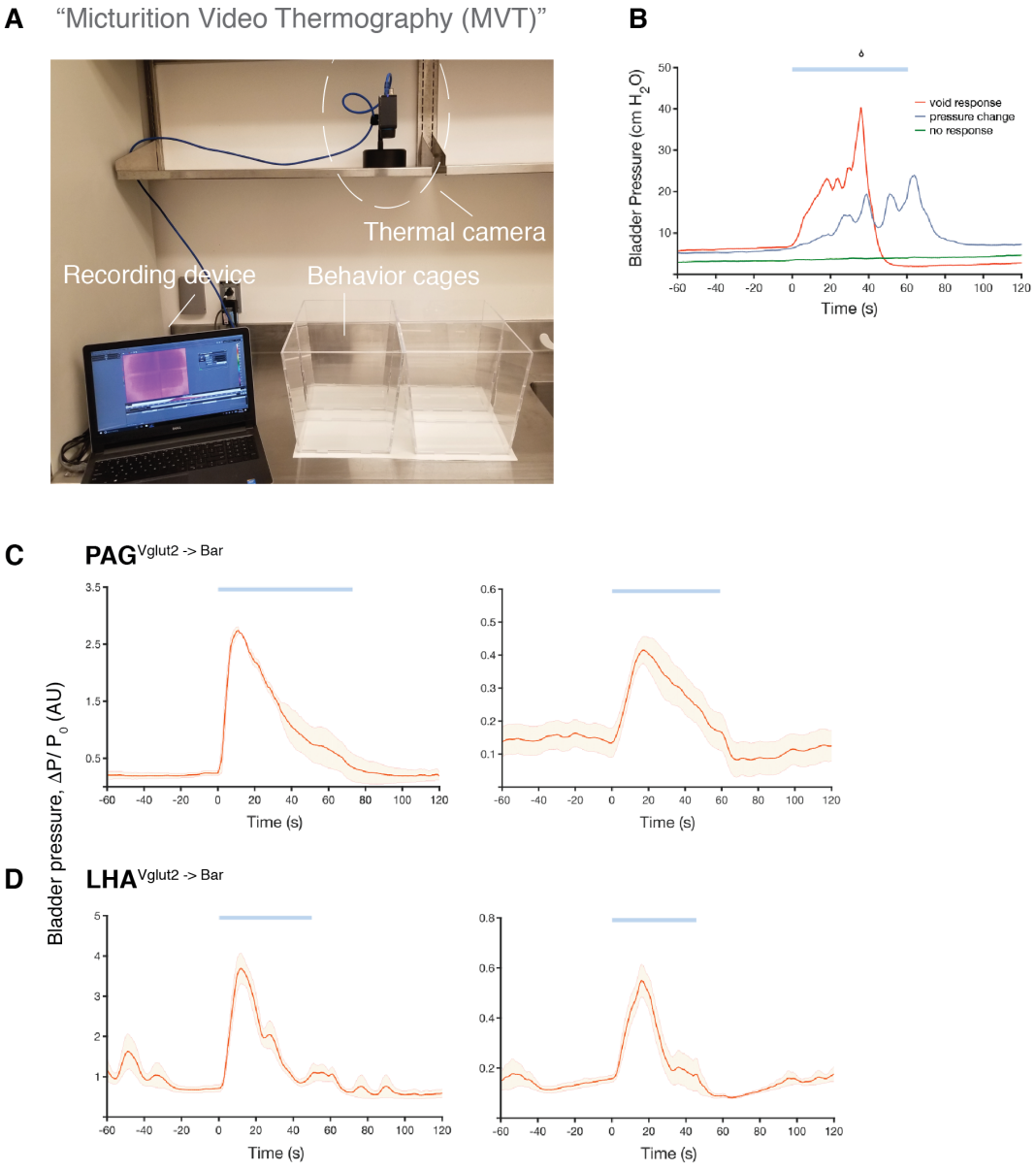

Figure S2. Optogenetic activation of excitatory Bar afferents leads to void responses and increased bladder pressure. Related to STAR Methods.

A) Micturition Video Thermography (MVT) setup for recording awake mice. The setup consists of a FLIR A65 thermal imaging temperature sensor positioned over the center of (up to) four plexiglass behavior boxes atop filter paper.

B) Example traces of bladder pressure on CMG, before and during and after optogenetic stimulations. Green line: contraction with void, red line: contraction with no void, blue line: no pressure change. Droplet icon indicates voiding contraction leading to a void.

C) Averaged CMG bladder pressure traces, before, during and after optogenetic stimulation (blue line; 10 Hz, 5 ms) that resulted in a pressure change with a void, from 2 different anesthetized *Vglut2-IRES-Cre* mice with AAV.DIO.ChR2 injected in PAG. Left and right, the data is an average of 3 and 12 micturition events, respectively.

D) Averaged CMG bladder pressure traces, before, during and after optogenetic stimulation (blue line; 10 Hz, 5 ms) that resulted in a pressure change with a void, from 2 different anesthetized *Vglut2-IRES-Cre* mice with AAV.DIO.ChR2 injected in LHA. Left and right, the data is an average of 15 and 17 micturition events. The shade in the graph represents the standard error of the mean.

Abbreviations: Bar, Barrington's Nucleus; ChR2, Channelrhodopsin2; CMG, cystometrogram; LHA, lateral hypothalamic area; MVT, Micturition Video Thermography 'awake void spot assay'; PAG, periaqueductal gray.

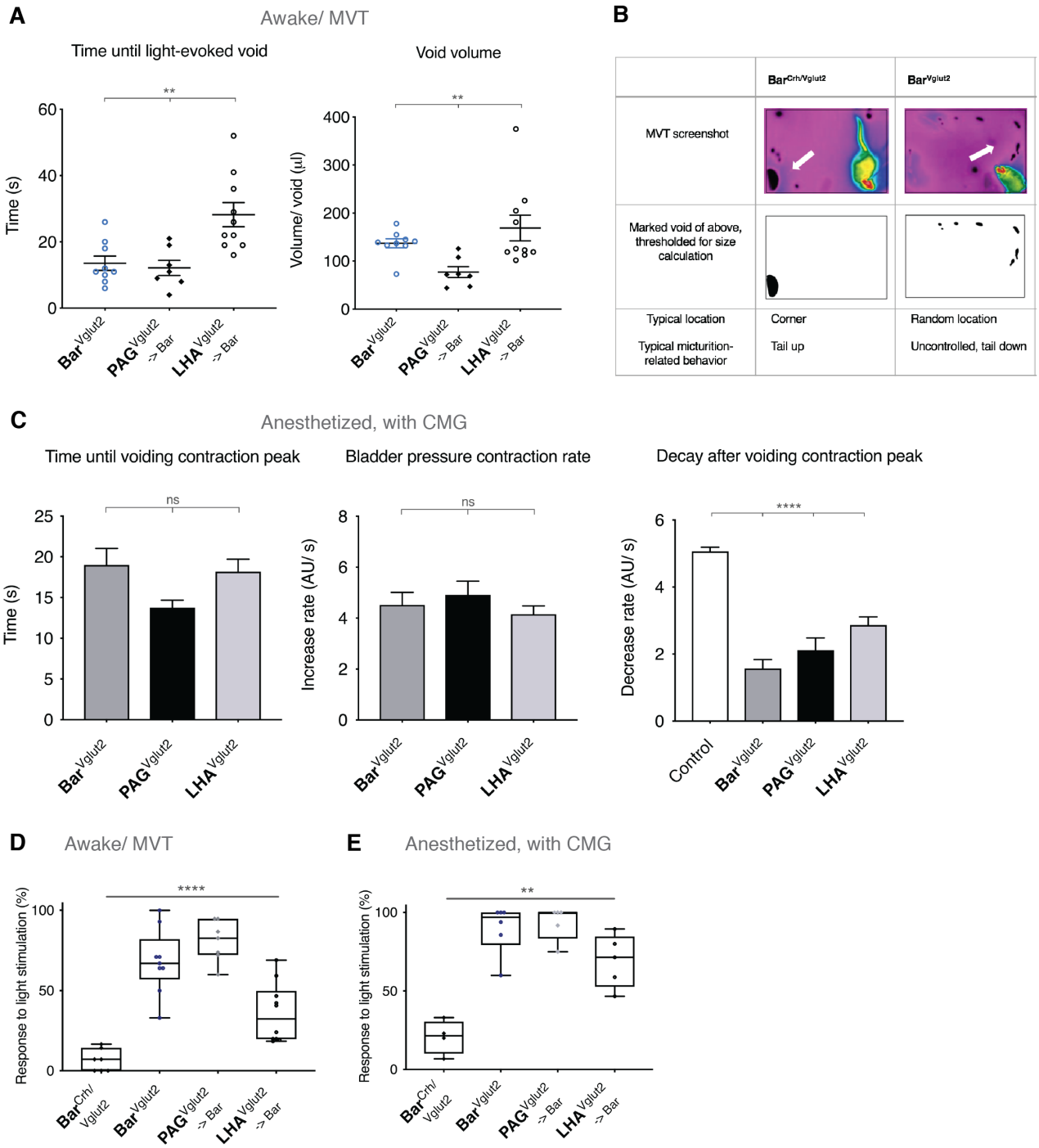
A
Awake/ MVT
Time until light-evoked void
Void volume
Time (s)
Volume/ void (µl)
**
**
Bar Vglut2
PAG Vglut2 -> Bar
LHA Vglut2 -> Bar
B
Bar Crh/Vglut2
Bar Vglut2
MVT screenshot
Marked void of above, thresholded for size calculation
Typical location
Corner
Random location
Typical micturition-related behavior
Tail up
Uncontrolled, tail down
C
Anesthetized, with CMG
Time until voiding contraction peak
Bladder pressure contraction rate
Decay after voiding contraction peak
Time (s)
Increase rate (AU/ s)
Decrease rate (AU/ s)
ns
ns
****
Control
D
Awake/ MVT
E
Anesthetized, with CMG
Response to light stimulation (%)
****
**

Figure S3. Micturition-related behaviors and detrusor activity with optogenetic light stimulation of glutamatergic neurons or axon terminals. Related to Figure 3 and 4.

A) Left graph: Averaged time until a light-evoked void from stimulation start, for Bar^{Vglut2}, $PAG^{Vglut2 \text{ -> } Bar}$ and $LHA^{Vglut2 \text{ -> } Bar}$ in awake mice. Kruskal-Wallis test ANOVA; ** p = 0.0024, followed by Dunn's test for multiple comparisons; *, p = 0.0113 and **, p = 0.0083 for Bar^{Vglut2} and $PAG^{Vglut2 \text{ -> } Bar}$ respectively, vs. $LHA^{Vglut2 \text{ -> } Bar}$. Data are presented as mean ± s.e.m. in individual mice, Bar^{Vglut2}, 85 events in 9 mice; PAG^{Vglut2}, 120 events in 7 mice; LHA^{Vglut2}, 101 events in 10 mice.
Right graph: Averaged volume per void of a light-evoked void, for Bar^{Vglut2}, $PAG^{Vglut2 \text{ -> } Bar}$ and $LHA^{Vglut2 \text{ -> } Bar}$ in awake mice. Kruskal-Wallis test ANOVA; ** p = 0.0038, followed by Dunn's test for multiple comparisons; **, p = 0.0067 and *, p = 0.0128 for Bar^{Vglut2} and $LHA^{Vglut2 \text{ -> } Bar}$ respectively, vs. $PAG^{Vglut2 \text{ -> } Bar}$.
B) Screenshot images of a video thermography recording. Arrows point to a light-evoked void during a stimulation trial. Below the screenshot is the indicated void of above, thresholded for void volume calculation.
The lower row: typical location of a light-evoked void per condition, and typical behavior observed.
C) Time until voiding contraction peak with light-stimulation (left panel) and bladder pressure contraction rate from start of light stimulation until voiding contraction peak (middle). One-way ANOVA followed by Tukey's test for multiple comparisons; ns for both.
Right panel: pressure decrease in 15 seconds post light-evoked void contraction peak. One-way ANOVA; ****, $p < 0.0001$, followed by Dunnett's test for multiple comparisons; ****, $p < 0.0001$ for Bar^{Vglut2}, $PAG^{Vglut2 \text{ -> } Bar}$ and $LHA^{Vglut2 \text{ -> } Bar}$. Data are presented as sample mean ± s.e.m., n = $Bar^{Control}$), 29 spontaneous void events without light stimulation in 3 mice; Bar^{Vglut2}, 31 light-evoked void events in 6 mice; $PAG^{Vglut2 \text{ -> } Bar}$, 25 light-evoked void events in 4 mice; $LHA^{Vglut2 \text{ -> } Bar}$, 51 light-evoked void events in 5 mice.
D) Likelihood of a micturition event following optogenetic stimulation of $Bar^{Crh/Vglut2}$ neurons in awake mice ('Awake'; n = 7 mice, 82 stimulations, 17-23/ mouse), of Bar^{Vglut2} neurons (n = 9 mice, 122 stimulations, 12-20/ mouse), of $PAG^{Vglut2 \text{ -> } Bar}$ axon terminals in awake mice (n = 7 mice, 150 stimulations, 19-36/ mouse), of $LHA^{Vglut2 \text{ -> } Bar}$ axon terminals in awake mice (n = 10 mice, 285 stimulations, 26-31/ mouse). Kruskal-Wallis test ANOVA; ****, $p < 0.0001$, followed by Dunn's test for multiple comparisons; ***, p = 0.0007 for $Bar^{Crh/Vglut2}$ vs. Bar^{Vglut2}; ****, $p < 0.0001$ and *, p = 0.0221 for $Bar^{Crh/Vglut2}$ and $LHA^{Vglut2 \text{ -> } Bar}$ respectively, vs. $PAG^{Vglut2 \text{ -> } Bar}$.
E) Likelihood of a micturition event following optogenetic stimulation of $Bar^{Crh/Vglut2}$ neurons in anesthetized mice ('Anesthetized/ CMG'; n = 4 mice, 45 stimulations, 6-16/ mouse), of Bar^{Vglut2} neurons (n = 6 mice, 43 stimulations, 5-10/ mouse), of $PAG^{Vglut2 \text{ -> } Bar}$ axon terminals in anesthetized mice (n = 5 mice, 31 stimulations, 2-12/ mouse), of $LHA^{Vglut2 \text{ -> } Bar}$ axon terminals in anesthetized mice (n = 5 mice, 87 stimulations,15-21/ mouse). Data are represented as medians with min to max values. Kruskal-Wallis test ANOVA; ** p = 0.0039, followed by Dunn's test for multiple comparisons, *, p = 0.0127 and **, p = 0.0093 for $Bar^{Crh/Vglut2}$ vs. Bar^{Vglut2} and $PAG^{Vglut2 \text{ -> } Bar}$ respectively.

Abbreviations: Bar, Barrington's Nucleus; CMG, cystometrogram; MVT, Micturition Video Thermography; LHA, lateral hypothalamic area; ns, not significant; PAG, periaqueductal gray.

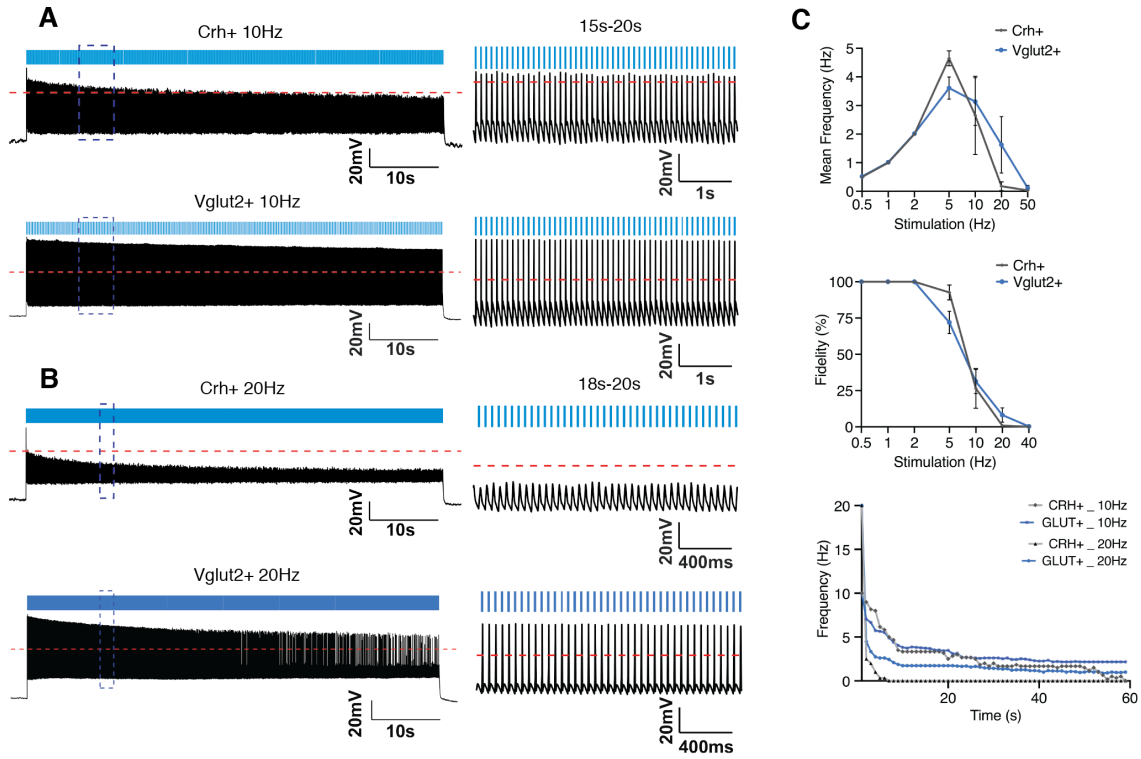
A
Crh+ 10Hz
15s-20s
20mV
10s
1s
Vglut2+ 10Hz
B
Crh+ 20Hz
18s-20s
400ms
Vglut2+ 20Hz
C
Crh+
Vglut2+
Mean Frequency (Hz)
Stimulation (Hz)
Fidelity (%)
CRH+ _ 10Hz
GLUT+ _ 10Hz
CRH+ _ 20Hz
GLUT+ _ 20Hz
Frequency (Hz)
Time (s)

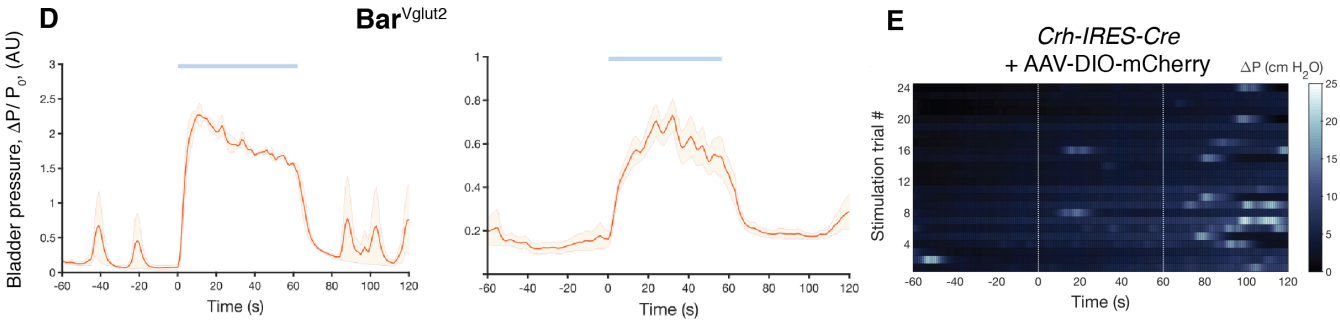
D
Bar Vglut2
Bladder pressure, ΔP/ P0, (AU)
Time (s)
E
Crh-IRES-Cre
+ AAV-DIO-mCherry
ΔP (cm H2O)
Stimulation trial #
Time (s)

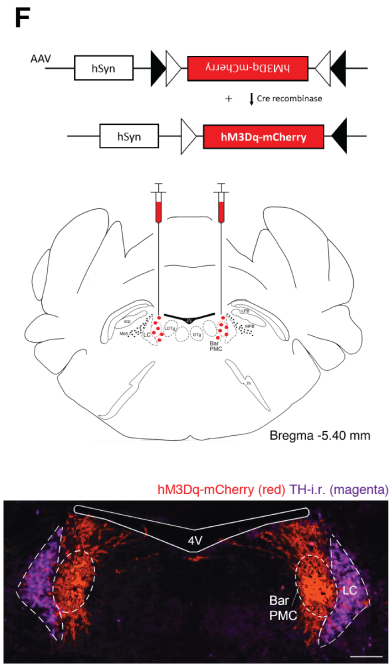
F
AAV
hSyn
hM3Dq-mCherry
Cre recombinase
Bregma -5.40 mm
hM3Dq-mCherry (red) TH-i.r. (magenta)
4V
Bar
PMC
LC

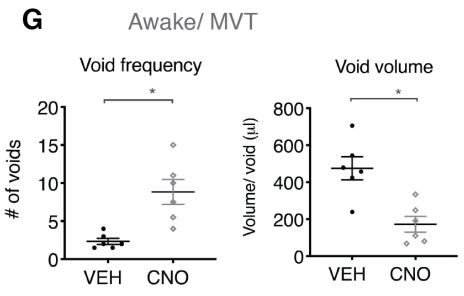
G
Awake/ MVT
Void frequency
# of voids
VEH
CNO
Void volume
Volume/ void (μl)

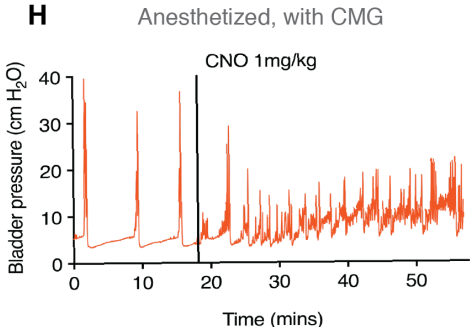
H
Anesthetized, with CMG
CNO 1mg/kg
Bladder pressure (cm H2O)
Time (mins)

Figure S4. Activation of neuron subpopulations in Bar triggers micturition behavior. Related to Figure 4.

A) Left panels: sample traces of a $Bar^{Crh/Vglut2}$ (upper left panel) and a Bar^{Vglut2} (lower left panel) neuron in response to 10 Hz of light stimulation *in vitro*. Right panels: magnification of the blue boxed portion (15s-20s).
B) Left panels: sample traces of a $Bar^{Crh/Vglut2}$ (upper left panel) and a Bar^{Vglut2} (lower left panel) neuron in response to 20 Hz of light stimulation (n = 6 cells for Crh, n = 23 cells for Vglut2). Right panels, magnification of the blue boxed portion (18s-20s).
C) Upper panel: The mean frequency of action potential firing of $Bar^{Crh/Vglut2}$ and Bar^{Vglut2} neurons in response to photostimulation. Middle: Spike fidelity in response to light pulse stimulation of $Bar^{Crh/Vglut2}$ and Bar^{Vglut2} neurons. Lower: Changes in frequency of action potentials firing of $Bar^{Crh/Vglut2}$ and Bar^{Vglut2} neurons during 1 min train of photostimulation at 10 Hz and 20 Hz.
D) Averaged CMG bladder pressure traces, before, during and after optogenetic stimulation (blue line; 10 Hz, 5 ms), from 2 different anesthetized *Vglut2-IRES-Cre* mice with AAV.DIO.ChR2 injected in Bar. Left and right graphs include 3 and 8 micturition events during light stimulation. The shade in the graph represents the standard error of the mean.
E) Heatmap showing ΔP before, during and after optogenetic stimulation (stimulus onset at time = 0s) from one control mouse. White dashed lines represent stimulus onset and offset.
F) Schematic of hM3Dq.mCherry construct targeted bilaterally to Bar in *Crh-IRES-Cre* mice. Lower panel: hM3Dq.mCherry expressing Bar^{Crh} neurons (red), and TH-i.r. labeled neurons (magenta) at the level of Bar.
G) Frequency of voiding (left graph) and averaged volume per void (right), following hM3Dq activation with VEH or CNO administration (1 mg/ kg i.p.) of $Bar^{Crh/Vglut2}$ neurons during 2-hour video thermography recordings. Wilcoxon matched-pairs signed rank test; *, p = 0.0312 (for frequency and for voided volume), n = 6 mice. Data are presented as population mean $\pm$ s.e.m.
H) A typical cystometrogram (CMG) bladder pressure trace, before and after CNO administration (1 mg/ kg i.p.), and activation of Bar^{Crh} neurons in an anesthetized *Crh-IRES-Cre* mouse.

Scale bar is 200 μm. *Abbreviations: 4V, 4th ventricle; Bar, Barrington's Nucleus; ChR2, Channelrhodopsin2; CMG, cystometrogram; CNO, Clozapine-N-Oxide; i.r., immunoreactive; LC, locus coeruleus; MVT, Micturition Video Thermography; PMC, pontine micturition center; TH, tyrosine hydroxylase; VEH, vehicle.*

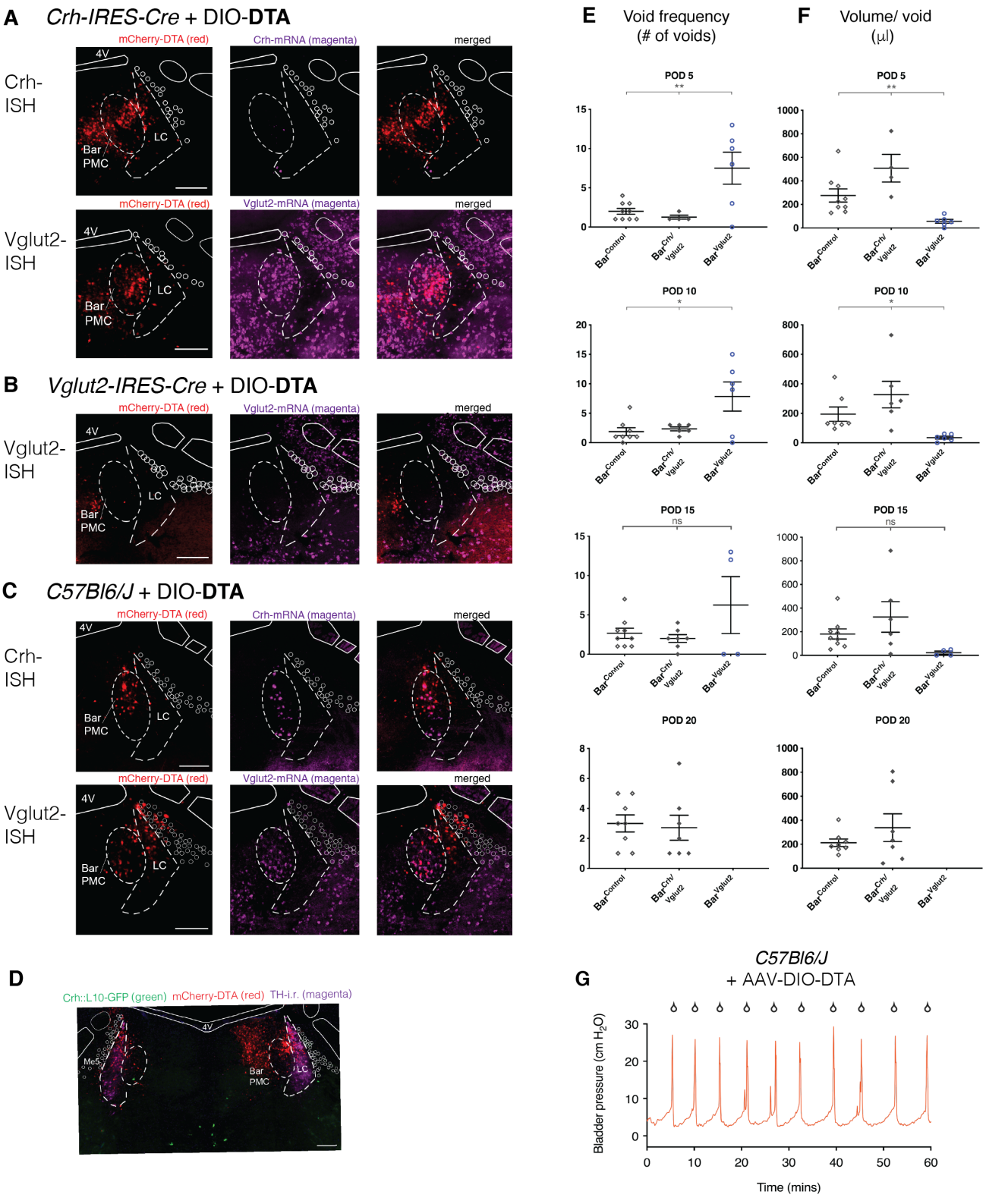
A
Crh-IRES-Cre + DIO-DTA
mCherry-DTA (red)
Crh-mRNA (magenta)
merged
Crh-ISH
Vglut2-mRNA (magenta)
Vglut2-ISH
4V
LC
Bar
PMC
B
Vglut2-IRES-Cre + DIO-DTA
C
C57Bl6/J + DIO-DTA
D
Crh::L10-GFP (green)
TH-i.r. (magenta)
Me5
E
Void frequency
(# of voids)
F
Volume/ void
(µl)
POD 5
POD 10
POD 15
POD 20
**
*
ns
BarControl
BarCrh/Vglut2
BarVglut2
G
C57Bl6/J
+ AAV-DIO-DTA
Bladder pressure (cm H2O)
Time (mins)

Figure S5. Selective ablation of glutamatergic or glutamatergic-Crh+ Bar neurons causes retention or delays voiding contractions. Related to Figure 5.

A) In a *Crh-IRES-Cre* mouse (left to right): mCherry.DTA (red) targeted to $Bar^{Crh/Vglut2}$ neurons, expression of mRNA for Crh (upper; magenta) or mRNA for Vglut2 (lower; magenta), and merged image.
B) In a *Vglut2-IRES-Cre* mouse (left to right): Bar neurons targeted with mCherry.DTA (red), Vglut2 mRNA expression (magenta), and merged image.
C) In a *C57Bl6* mouse (left to right): Bar neurons targeted with mCherry.DTA (red), mRNA for Crh (upper; magenta) or mRNA for Vglut2 expression (lower; magenta), and merged image.
D) DIO-DTA transduced neurons (red), remaining Crh-expressing neurons (green) ventral to the injection site, and TH-i.r. labeled neurons (magenta) at the level of the PMC.
E) Frequency of voiding during a 2-hour video thermography awake behavior recording on POD 5, 10, 15 or 20. Data is represented as population mean ± s.e.m. for *C57Bl6/J* ($Bar^{Control}$, n = 9 mice), *Crh-IRES-Cre* ($Bar^{Crh/Vglut2}$, n = 7 mice) and *Vglut2-IRES-Cre* (Bar^{Vglut2}, n = 4 mice) injected bilaterally with DIO-DTA. RM one-way ANOVA; POD 5; **, p = 0.0039, with Dunnett's multiple comparisons test; **, p = 0.0048 control vs. Bar^{Vglut2}; POD 10; *, p = 0.013; and with Dunnett's multiple comparisons test; *, p = 0.011 control vs. Bar^{Vglut2}; POD 15; ns.
F) Volume per void during a 2-hour video thermography awake behavior recording on POD 5, 10, 15 or 20. Data is represented as population mean ± s.e.m. for *C57Bl6/J* ($Bar^{Control}$, n = 9 mice), *Crh-IRES-Cre* ($Bar^{Crh/Vglut2}$, n = 7 mice) and *Vglut2-IRES-Cre* (Bar^{Vglut2}, n = 4 mice) injected bilaterally with DIO-DTA. RM one-way ANOVA; POD 5; **, p = 0.0016, with Dunnett's multiple comparisons test; *, p = 0.0482 and *, p = 0.0326 for control vs. Bar^{Crh} and Bar^{Vglut2} respectively; POD 10; *, p = 0.0118 and POD 15; ns.
G) A representative CMG bladder pressure trace recorded in an anesthetized *C57Bl6* control mouse with DIO-DTA virally targeted to Bar.

Scale bar is 200 μm. Droplet icon indicates voiding contraction leading to a void. *Abbreviations: 4V, 4th ventricle; Bar, Barrington's Nucleus; DTA, diphtheria toxin-subunit A; i.r., immunoreactive; ISH, In Situ Hybridization; LC, locus coeruleus; ns, not significant; PMC, pontine micturition center; POD, post-operative day; TH, tyrosine hydroxylase.*

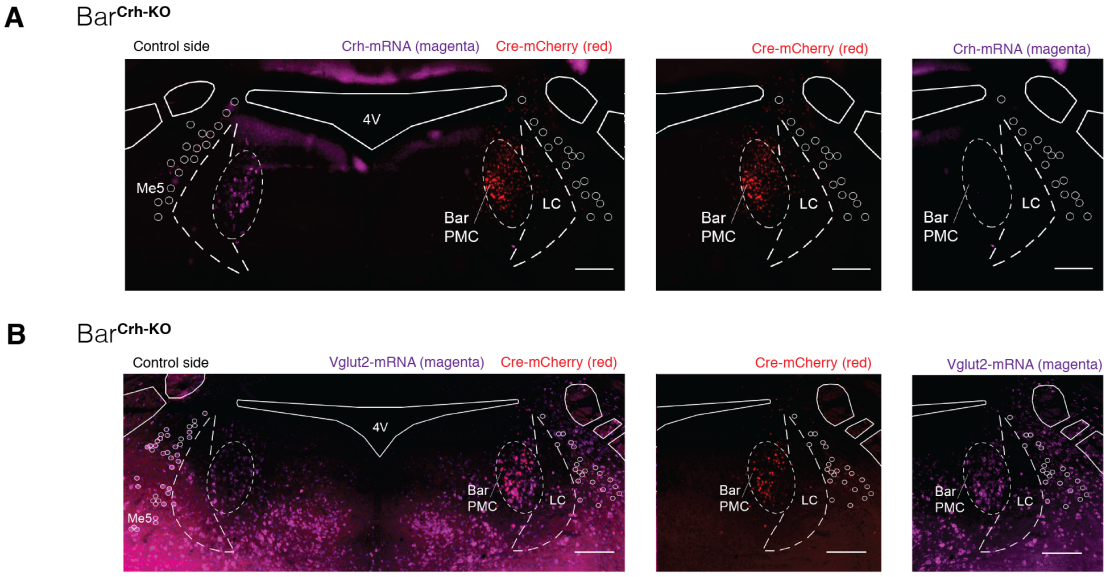

Figure S6. Deleting Crh from Bar neurons does not affect voiding behavior significantly Related to Figure 6.

A) AAV.Cre.mCherry injected unilaterally in Bar of $Crh^{fl/fl}$ mice. Left panel: merged image showing control and injected side (red), with Crh-mRNA in magenta. AAV.Cre.mCherry (red) targeted to Bar (middle), and Crh-mRNA (magenta; right).

B) AAV.Cre.mCherry injected unilaterally in Bar of $Crh^{fl/fl}$ mice. Left panel: merged image showing control and injected side (red), with Vglut2-mRNA in magenta. AAV.Cre.mCherry (red) targeted to Bar (middle), and Vglut2-mRNA (magenta; right).

Scale bar is 200 μm. *Abbreviations: 4V, 4th ventricle; Bar, Barrington's nucleus; KO, knockout; LC, locus coeruleus; PMC, pontine micturition center.*